

Biexcitons in coupled quantum dots as a source of entangled photons

Oliver Gywat, Guido Burkard, and Daniel Loss

Department of Physics and Astronomy, Klingelbergstrasse 82, CH-4056 Basel, Switzerland

(Received 5 February 2002; published 22 May 2002)

We study biexcitonic states in two tunnel-coupled semiconductor quantum dots and show that such systems provide the possibility to produce polarization-entangled photons or spin-entangled electrons that are spatially separated at production. We distinguish between the various spin configurations and calculate the low-energy biexciton spectrum using the Heitler-London approximation as a function of magnetic and electric fields. The oscillator strengths for the biexciton recombination involving the sequential emission of two photons are calculated. The entanglement of the photon polarizations resulting from the spin configuration in the biexciton states is quantified as a function of the photon emission angles.

DOI: 10.1103/PhysRevB.65.205329

PACS number(s): 78.67.Hc, 71.35.-y, 72.25.Fe, 73.21.La

Entanglement has been identified as an essential resource for many applications in the recently developed field of quantum communication and quantum computation.¹ Several quantum communication schemes have already been successfully implemented with pairs of polarization-entangled photons produced by parametric downconversion,¹ e.g., the faithful transmission of a quantum state (quantum teleportation), entanglement-assisted classical communication (e.g., quantum superdense coding), and the production of a secure cryptographic key (quantum key distribution). Recently, there has also been growing interest in solid-state implementations of quantum computation using the electron spin as the qubit,² as well as quantum communication with spin-entangled electrons. Superconductor-normal junctions in combination with quantum dots (QDs) have been suggested as a device for producing entangled electrons.³ Still, the efficient and deterministic production of both entangled photons and electrons poses a theoretical and experimental challenge. In the case of photons, the use of electron-hole recombination in a single QD was recently suggested.^{4,5} Nonresonant excitation of a QD is expected to produce pairs of entangled photons with an efficiency (production rate/pump rate) that is about four orders of magnitude bigger than for parametric downconversion.⁵

In this paper, we study the production of polarization-entangled photons, or, alternatively, spin-entangled electrons, using the biexcitonic ground state in *two tunnel-coupled* QDs. For this purpose we study the low-energy biexcitonic states in coupled QDs, determining their energy spectrum and their optical properties in the presence of external magnetic and electric fields. We concentrate on the spin configuration of the calculated states, being related to the orbital wave function via the Fermi statistics that is implemented in a Heitler-London (HL) ansatz for electrons and for holes. As a special quality of a double dot, we find that in the (spin-entangled) biexcitonic ground state, the biexciton favors a configuration with each QD occupied by one exciton, thus providing a basis for the separation of the entangled particles. Even though coupled QDs are usually separated by a distance less than the wavelength of the emitted light, it might still be possible to directly detect the photons at separate locations. It can, e.g., be expected that due to anisotropies the two dots have different preferred emission directions

enclosing a fixed angle. Two subsequent photons, which are emitted with a time delay given by the exciton lifetime, could then be detected separately in the far field.

In contrast to our calculations, earlier studies for quantum computation or entanglement production with excitons in QDs concentrate on single QDs (Refs. 4–8) and/or on charge degrees of freedom (neglecting spin).^{6–11} Also, instead of a pure electrostatic interdot coupling,^{9,11} we take into account the tunneling of electrons and holes between the coupled QDs.

Biexcitons consist of two bound excitons that themselves are formed by a conduction-band electron and a valence-band hole in a semiconductor, bound together by the attractive Coulomb interaction. Following the theory of excitonic absorption in single QDs,¹² the biexcitonic states in single QDs have been investigated^{13–20} and single excitons in coupled QDs have been observed in experiment.^{10,21} Recently, spin spectroscopy of excitons in QDs was performed using polarization-resolved magnetophotoluminescence.²² Two regimes can be distinguished in the discussion of excitons confined in QDs.¹² In the *weak confinement* limit $a_X \ll a_e, a_h$, where a_X is the radius of the free exciton and a_e, a_h the electron and hole effective Bohr radii in the QD, an exciton can (as in the bulk material) be considered as a boson in an external confinement potential. In the case of *strong confinement* $a_X \gg a_e, a_h$, electrons and holes are separately confined in the QD and the bosonic nature of the electron-hole pair breaks down. Since, e.g., in bulk GaAs $a_X \approx 10$ nm, we are in an intermediate regime $a_X \approx a_e, a_h$ for typical QD radii. Here, we start from a strong confinement ansatz, i.e., from independent electrons and holes (two of each species), and then use the HL approximation to include the Coulomb interaction and the tunneling. Unlike for bulk biexcitons, where the HL approximation fails for some values of $\xi = m_e/m_h$,²³ we are here in a different situation—much more similar to the H₂ molecule—because the single particle orbitals are defined by the strong QD confinement, the latter playing the role of the (“infinitely” heavy) protons of the H₂ molecule.

We obtain the low-energy (spin-resolved) biexciton spectrum in which the electrons and holes each form either a spin singlet or triplet. Subsequently, we calculate the oscillator strength, being a measure for the optical transition rates. The

spin of the biexciton states relates to two different states of the polarization-entangled photon pair produced in the recombination. We quantify the entanglement of the photon pair depending on the emission directions. The variation of the spectrum and the oscillator strengths due to magnetic or electric fields allows to use ground-state biexcitons in tunnel-coupled QDs as a pulsed source of entangled photon pairs.

We model the biexciton (two electrons and two holes) in two coupled QDs by the Hamiltonian

$$H = \sum_{\alpha=e,h} \sum_{i=1}^2 h_{\alpha i} + H_C + H_Z + H_E, \quad (1)$$

where $h_{\alpha i} = [\mathbf{p}_{\alpha i} + q_{\alpha} \mathbf{A}(\mathbf{r}_{\alpha i})/c]^2/2m_{\alpha} + V_{\alpha}(\mathbf{r}_{\alpha i})$ is the single-particle Hamiltonian for the i th electron ($\alpha=e, q_e = -e$) or hole ($\alpha=h, q_h = +e$) in two dimensions with coordinate $\mathbf{r}_{\alpha i}$ and spin $\mathbf{S}^{\alpha i}$. The potential $V_{\alpha}(x, y) = m_{\alpha} \omega_{\alpha}^2 [(x^2 - a^2)^2/4a^2 + y^2]/2$ describes two QDs centered at $(x = \pm a, y = 0)$, separated by a barrier of height $m_{\alpha} \omega_{\alpha}^2 a^2/8$. Electrons and holes have effective masses m_{α} and confinement energies $\hbar \omega_{\alpha}$. The Coulomb interaction is included by $H_C = (1/2) \sum_{(\alpha, i) \neq (\beta, j)} q_{\alpha} q_{\beta} / \kappa |\mathbf{r}_{\alpha i} - \mathbf{r}_{\beta j}|$, with a dielectric constant κ (for bulk GaAs, $\kappa = 13.18$). A magnetic field \mathbf{B} in z direction leads to orbital effects via the vector potential (in the symmetric gauge) $\mathbf{A} = B(-y, x, 0)/2$ and to the Zeeman term $H_Z = \sum_{\alpha, i} g_{\alpha} \mu_B B S_z^{\alpha i}$, where g_{α} is the effective g factor of the electron (hole) and μ_B is the Bohr magneton. Restricting ourselves to the low-energy physics of QDs filled with few particles, we can assume approximately two-dimensional (2D) parabolic confinement. We assume the simultaneous confinement of electrons and holes which can be realized, e.g., in QDs formed by thickness fluctuations in a quantum well⁸ or by self-assembled QDs.^{24,25} A particle in a single QD is thus described by the Fock-Darwin (FD) Hamiltonian $h_{\alpha}^{\pm a}(\mathbf{r}_{\alpha i})$,²⁶ comprising a harmonic potential $v_{\alpha}^{\pm a}(\mathbf{r}) = m_{\alpha} \omega_{\alpha}^2 [(x \mp a)^2 + y^2]/2$ and a perpendicular magnetic field. In prospect of the HL ansatz below we write the single-particle part of the Hamiltonian Eq. (1) as $\sum_{\alpha} [h_{\alpha}^{-a}(\mathbf{r}_{\alpha 1}) + h_{\alpha}^{+a}(\mathbf{r}_{\alpha 2})] + H_W(\{\mathbf{r}_{\alpha i}\}) \equiv H_0 + H_W$, where $H_W(\{\mathbf{r}_{\alpha i}\}) = \sum_{\alpha} [\sum_i V_{\alpha}(\mathbf{r}_{\alpha i}) - v_{\alpha}^{-a}(\mathbf{r}_{\alpha 1}) - v_{\alpha}^{+a}(\mathbf{r}_{\alpha 2})]$. An in-plane electric field $\mathbf{E} = \varepsilon \hat{\mathbf{y}}$ is described by $H_E = e\varepsilon(y_{e1} + y_{e2} - y_{h1} - y_{h2})$ and can be included in H_0 . We put $\varepsilon = 0$ here and discuss the case $\varepsilon \neq 0$ below.

The valence band is assumed to be split into well-separated heavy and light hole bands and only heavy-hole excitations are considered in the following. The FD ground states $|D\rangle_{\alpha}$ in the QD $D=1,2$, which are used to make a *variational* HL ansatz are²⁶

$$\langle \mathbf{r} | D \rangle_{\alpha} = \sqrt{\frac{b_{\alpha}}{\pi a_{\alpha}^2}} \exp\left(-\frac{b_{\alpha}}{2a_{\alpha}^2} [(x \pm a)^2 + y^2] \pm \frac{i q_{\alpha} a y}{2e l_B^2}\right), \quad (2)$$

where the upper (lower) sign holds for $D=1(2)$, $l_B = \sqrt{\hbar c/eB}$, and $b_{\alpha} = \sqrt{1 + (eB/2cm_{\alpha}\omega_{\alpha})^2}$.

We now make a strong confinement ansatz by constructing two-particle orbital wave functions for electrons and for holes separately according to the HL method, i.e., a symmet-

ric ($|s\rangle^{\alpha} \equiv |I=0\rangle^{\alpha}$, spin singlet) and an antisymmetric ($|t\rangle^{\alpha} \equiv |I=1\rangle^{\alpha}$, spin triplet) linear combination of two-particle states $|DD'\rangle_{\alpha} = |D\rangle_{\alpha} \otimes |D'\rangle_{\alpha}$,

$$|I\rangle^{\alpha} = N_{\alpha I} [|12\rangle_{\alpha} + (-1)^I |21\rangle_{\alpha}], \quad (3)$$

where $N_{\alpha I} = 1/\sqrt{2(1 + (-1)^I |S_{\alpha}|^2)}$ and $S_{\alpha} = \langle 1|2\rangle_{\alpha}$ denotes the overlap (or tunneling amplitude) between the two orbital wave functions $|1\rangle_{\alpha}$ and $|2\rangle_{\alpha}$. We continue by forming the four biexciton states $|IJ\rangle = |I\rangle^e \otimes |J\rangle^h$, where $I=0$ (1) for the electron singlet (triplet) and $J=0$ (1) for the hole singlet (triplet). The energies

$$E_{IJ} = \langle IJ | H | IJ \rangle = E^0 + E^Z + E_{IJ}^W + E_{IJ}^C, \quad (4)$$

with $E_{IJ}^A \equiv \langle IJ | H_A | IJ \rangle$, can be calculated analytically. In units of $\hbar \omega_e$, we find $E_0 \equiv E_{IJ}^0 = 2(b_e + b_h/\eta)$, where $\eta = \omega_e/\omega_h$, $E^Z \equiv E_{IJ}^Z = (\mu_B B/\hbar \omega_e) \sum_{\alpha i} g_{\alpha} S_z^{\alpha i}$, and

$$E_{IJ}^W = \frac{3}{16d^2} \left(\frac{1}{b_e^2} + \frac{\xi}{b_h^2} \right) - \frac{3d^2}{4} \left(1 + \frac{1}{\xi \eta^2} \right) + 3N_{IJ} \left[d^2 \left(1 + \frac{1}{\xi \eta^2} \right) + (-1)^J S_h^2 \left(d^2 - \frac{1}{\eta b_h} \right) + (-1)^I S_e^2 \left(\frac{d^2}{\xi \eta^2} - \frac{1}{b_e} \right) - (-1)^{I+J} S_e^2 S_h^2 \left(\frac{1}{b_e} + \frac{1}{\eta b_h} \right) \right], \quad (5)$$

where $2d = 2a/a_e$ is the dimensionless interdot distance, $a_e = \sqrt{\hbar/m_e \omega_e}$ is the electronic Bohr radius, $S_e = \exp(-d^2[2b_e - 1/b_e])$, $S_h = \exp(-d^2[2b_h - 1/b_h]/\xi \eta)$, $N_{IJ} = N_e^I N_h^J$, and $\xi = m_e/m_h$. For E_{IJ}^C , we find

$$E_{IJ}^C = \frac{E_{ee} + (-1)^I \tilde{E}_{ee}}{1 + (-1)^I S_e^2} + \frac{E_{hh} + (-1)^J \tilde{E}_{hh}}{1 + (-1)^J S_h^2} + 8N_{IJ} [E_X + E_{eh} + (-1)^I S_e \tilde{E}_{Xe} + (-1)^J S_h \tilde{E}_{Xh} + (-1)^{I+J} S_e S_h \tilde{E}_{Xeh}], \quad (6)$$

where we have used the abbreviations

$$E_{\alpha\alpha} = c \sqrt{b_{\alpha}/x_{\alpha}} \exp(-b_{\alpha} d^2/x_{\alpha}) I_0(b_{\alpha} d^2/x_{\alpha}), \quad (7)$$

$$\tilde{E}_{\alpha\alpha} = c \sqrt{\frac{b_{\alpha}}{x_{\alpha}}} S_{\alpha} \exp\left(-\frac{b_{\alpha} d^2}{x_{\alpha}}\right) I_0\left(\frac{d^2}{x_{\alpha}} \left[b_{\alpha} - \frac{1}{b_{\alpha}} \right]\right), \quad (8)$$

$$E_X = -c \sqrt{\bar{b}}, \quad (9)$$

$$E_{eh} = E_X \exp(-\bar{b} d^2) I_0(\bar{b} d^2), \quad (10)$$

$$\tilde{E}_{X\alpha} = 2S_{\alpha} E_X \exp(-\bar{b} d^2/4b_{\alpha}^2) I_0(\bar{b} d^2/4b_{\alpha}^2), \quad (11)$$

$$\tilde{E}_{Xeh} = S_e S_h E_X \{ \exp(\bar{b}_1 d^2/2) I_0(\bar{b}_1 d^2/2) + \exp(\bar{b}_2 d^2/2) I_0(\bar{b}_2 d^2/2) \}. \quad (12)$$

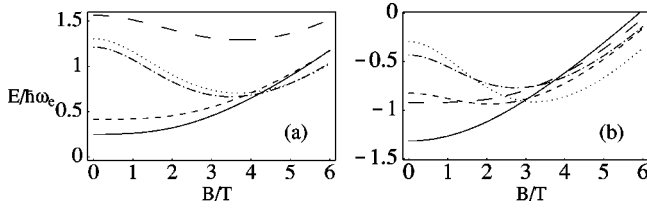


FIG. 1. Biexciton energies in units of $\hbar\omega_e$ for (a) $\eta = \omega_e/\omega_h = 1/2$, (b) $\eta = 1/\xi = 1.67$ ($a_e = a_h$), in a 2D GaAs system ($m_e = 0.067m_0$, $m_{hh} = 0.112m_0$), $\hbar\omega_e = 3$ meV, and $d = 0.7$. The plotted HL energies E_{IJ} are E_{ss} (solid line), E_{st} (short-dashed line), E_{ts} (dot-dashed line), and E_{tt} (dotted line), neglecting the Zeeman energy. The exchange splittings $E_{IJ} - E_{sJ}$, $J = s, t$, for electrons are larger than for holes ($E_{It} - E_{Is}$, $I = s, t$) in (a) where $\eta\xi < 1$, but of the same order in (b) ($\eta\xi = 1$). At $B = 0$, $|ss\rangle$ has the lowest energy, while for larger B , there is a crossover to a $|tt\rangle$ ground state. Double occupancy of a QD (long-dashed line) becomes more favorable with increasing η ; in (a), $\bar{E} > E_{IJ}$, $I, J = s, t$, while in (b), \bar{E} is smaller than some of the E_{IJ} for small B .

Here, $I_0(x)$ is the zeroth-order modified Bessel function, $c = e^2\sqrt{\pi/2}/\kappa a_e\hbar\omega_e$ is a dimensionless parameter characterizing the Coulomb interaction, $x_e = 1$, $x_h = \xi\eta$, $\bar{b} = 2b_e b_h / (b_h + \xi\eta b_e)$, $\bar{b}_1 = b_e - 1/b_e + [b_h - 1/b_h]/\xi\eta$, and $\bar{b}_2 = ([b_e - 1/b_e][b_h - 2\xi\eta b_e] + b_e[b_h - 1/b_h]) / (b_h + \xi\eta b_e)$. Figure 1 shows the biexciton energies E_{IJ} ($I, J = 0, 1 = s, t$) in the double QD as a function of an applied external magnetic field in z direction. The Zeeman interaction H_Z causes an additional level splitting of $\approx 0.02\hbar\omega_e/T$ (assuming $|g_e| \approx |g_h| \approx 1$) for the triplet states with $\sum_i S_z^{ai} \neq 0$ which is not shown in Fig. 1. The electron-hole exchange interaction for the GaAs QDs considered here is reported to be only on the order of tens of μeV (Ref. 27) and can therefore be neglected. The self-consistency of omitting excited single-QD states in the HL ansatz can be checked by comparing the energy $E_{IJ}^C + E_{IJ}^W$ to the single-QD level spacing. This criterion is fulfilled for interdot distances $2a \gtrsim 20$ nm. In addition to the HL states $|IJ\rangle$, we consider the double occupancy states $|DDDD\rangle$ for which all four particles are located on the same QD $D = 1, 2$. Their energies are given by $\bar{E} = E^0 + E^Z + \bar{E}^W + \bar{E}^C$, with $\bar{E}^W = 3(1/b_e^2 + \xi/b_h^2)/16d^2$, and $\bar{E}^C = c(\sqrt{b_e} + \sqrt{b_h/\xi\eta} - 4\sqrt{\bar{b}})$.

We proceed to the calculation of the oscillator strengths of biexciton-exciton and exciton-vacuum transitions. The oscillator strength f is a measure for the coupling of exciton states to the electromagnetic field and is proportional to the optical transition rates. For a transition between the $N+1$ and N exciton states $|N+1\rangle$ and $|N\rangle$, the oscillator strength is defined as

$$f_{N+1,N} = \frac{2|p_{N\kappa\lambda}|^2}{m_0\hbar\omega_{N+1,N}}, \quad (13)$$

where m_0 is the bare electron mass, $\hbar\omega_{N+1,N} = E_{N+1} - E_N$, and $p_{N\kappa\lambda} = \langle N+1 | \mathbf{e}_{\kappa\lambda} \cdot \mathbf{p} | N \rangle$, where $\mathbf{e}_{\kappa\lambda}$ is the unit polarization vector for a photon with momentum \mathbf{k} and helicity λ

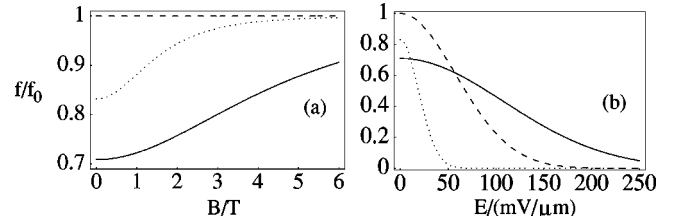


FIG. 2. Oscillator strength $f_{X,0}$ for GaAs QDs in units of f_0 as a function of (a) the magnetic field B (in T) at $E = 0$ and (b) the electric field E (in $\text{mV}/\mu\text{m}$) at $B = 0$, with $\eta = \omega_e/\omega_h = 1/2$ (solid line), $\eta = 1/\xi$ (dashed line), $\eta = 4$ (dotted line). For $\eta = 1/\xi$ the B field has no effect on C_{eh} .

$= \pm 1$, and \mathbf{p} is the electron momentum operator. For $p_{N\kappa\lambda}$ we find in the dipole approximation $a_\alpha \ll 2\pi/k$ ($a_\alpha \approx 20$ nm, $2\pi/k \approx 1$ μm),

$$p_{N\kappa\lambda} = [(N+1)!]^2 \sum_{\{\sigma_i, \tau_j\}, \sigma} M_{\sigma\lambda}(\theta) \int d^3r \prod_{i,j} d^3r_i d^3s_j \times \Phi_N(\{\mathbf{r}_i, \sigma_i\}; \{\mathbf{s}_j, \tau_j\}) \times \Phi_{N+1}^*(\{\mathbf{r}_i, \sigma_i\}, \mathbf{r}, \sigma; \{\mathbf{s}_j, \tau_j\}, \mathbf{r}, \sigma), \quad (14)$$

where Φ_N is the N -exciton wave function, depending on the conduction-band electron (valence-band hole) coordinates \mathbf{r}_i (\mathbf{s}_j) and their spins σ_i (τ_j) ($i, j = 1, \dots, N$). The coordinate and spin of the electron and the hole created or annihilated during the optical transition are denoted by \mathbf{r} and σ . The interband momentum matrix element for a cubic crystal symmetry is given by $M_{\sigma\lambda}(\theta) = \mathbf{e}_{\kappa\lambda} \cdot \mathbf{p}_{cv}(\sigma) = p_{cv}[\cos(\theta) - \sigma\lambda]/2 \equiv p_{cv}m_{\sigma\lambda}(\theta)$, where θ is the angle between \mathbf{k} and the normal to the plane of the 2D electron system (assuming that the latter coincides with one of the main axes of the cubic crystal), and $E_p = 2p_{cv}^2/m_0$ ($= 25.7$ eV for GaAs).

According to Eq. (14), the orbital momentum matrix element for transitions from the exciton vacuum $|0\rangle$ to an exciton state $|X\rangle = |D\rangle_e \otimes |D\rangle_h \equiv |DD\rangle$ in one QD (or for the optical recombination of $|X\rangle$) is $p_0 = M_{\sigma\lambda}(\theta) \int d^3r \Phi_1^*(\mathbf{r}, \mathbf{r}) \equiv M_{\sigma\lambda}(\theta) C_{eh}$. The exciton wave function is denoted by $\Phi_1(\mathbf{r}_e, \mathbf{r}_h) = \langle \mathbf{r}_e, \mathbf{r}_h | X \rangle$. From this, we find for the oscillator strength

$$f_{X,0} = \frac{2|p_0|^2}{m_0\hbar\omega_{X,0}} = \frac{E_p}{\hbar\omega_{X,0}} M_{\sigma\lambda}(\theta)^2 |C_{eh}|^2, \quad (15)$$

and $C_{eh} = 2\sqrt{\xi\eta b_e b_h / (b_h + \xi\eta b_e)}$. In Fig. 2(a) we plot $|C_{eh}|^2 = f/f_0$ as a function of the magnetic field, where $f_0 = E_p m_{\sigma\lambda}(\theta)^2 / E_g$ denotes the oscillator strength for (bulk) interband transitions, equating $\hbar\omega_{X,0}$ with the band-gap energy E_g . Since we have made a strong confinement ansatz, the obtained oscillator strength is independent of the QD volume V . For weak confinement, one would expect $f \propto V$. Figure 2(b) shows the suppression of the exciton transition rate by an electric field.

The momentum matrix element p_1 for transitions from an exciton state $|X\rangle$ to a biexciton state $|XX\rangle$ is given by $p_1 = -2M_{\sigma\lambda}(\theta) \int d^3r_e d^3r_h d^3r \Phi_2^*(\mathbf{r}_e, \mathbf{r}; \mathbf{r}_h, \mathbf{r}) \Phi_1(\mathbf{r}_e, \mathbf{r}_h)$. If the

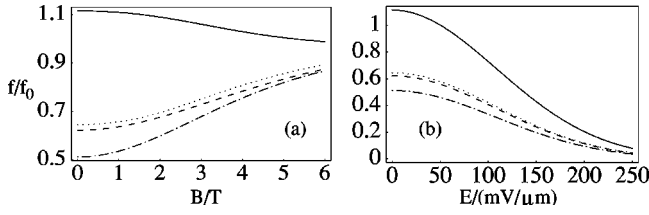


FIG. 3. Oscillator strengths $f_{XX,X}$ for transitions between the biexciton states $|XX\rangle=|IJ\rangle$ and a single remaining exciton on one QD in units of f_0 as a function of (a) the magnetic field B (in T) at $E=0$ and (b) the electric field E (in mV/ μm) at $B=0$. The parameters were chosen for GaAs with $\eta=\omega_e/\omega_h=1/2$. The line styles correspond to those for E_{IJ} in Fig. 1.

recombining electron and hole are on the same QD, the integral over \mathbf{r} yields C_{eh} , otherwise $S_{eh}=C_{eh}\exp\{-2d^2[b_e-\xi\eta/(b_h+\xi\eta b_e)]\}$.

We give here our result for p_1 for a transition between the HL biexciton states $|XX\rangle=|IJ\rangle$ with one exciton on each QD and a single exciton in the final state $|X\rangle=|DD\rangle$, a single exciton on dot $D=1,2$,

$$\begin{aligned} |\langle IJ|\mathbf{e}_{\mathbf{k}\lambda}\cdot\mathbf{p}|DD\rangle| &= 2M_{\sigma\lambda}(\theta)\sqrt{N_{IJ}}\{C_{eh}[(-1)^{I+J}+S_eS_h] \\ &+ S_{eh}[(-1)^J S_e+(-1)^I S_h]\}. \end{aligned} \quad (16)$$

Approximating $\hbar\omega_{XX,X}\approx E_g$, we plot the corresponding oscillator strength versus B and E in Figs. 3(a) and 3(b). Results for $f_{XX,X}$, also including the (biexciton) double occupancy state $|DDDD\rangle$ and various final (exciton) states, will be given elsewhere.²⁸

The main effect of an electric field is to spatially separate the electrons from the holes, which leads to a reduction of the oscillator strengths²⁸ [cf. Figs. 2(b) and 3(b)]. Hence, the optical transition rate can be efficiently switched off and on, thus allowing the deterministic emission of one photon pair.

Transformation of a HL biexciton state $|IJ\rangle$ into the basis of two coupled excitons yields a superposition of dark ($S_z=\pm 2$) and bright ($S_z=\pm 1$) exciton states. The emitted photon states are (up to normalization)

$$|\chi_{IJ}\rangle\propto|+1,\theta_1\rangle|-1,\theta_2\rangle+(-1)^{I+J}|-1,\theta_1\rangle|+1,\theta_2\rangle, \quad (17)$$

where $|\sigma,\theta\rangle=N(\theta)[m_{\sigma,+1}(\theta)|\sigma_+\rangle+m_{\sigma,-1}(\theta)|\sigma_-\rangle]$ is the state of a photon emitted from the recombination of an elec-

tron with spin $S_z=\sigma/2=\pm 1/2$ and a heavy hole with spin $S_z=3\sigma/2$ in a direction that encloses the angle θ with the normal to the plane of the 2D electron and hole motion. We assume here that the two emitted photons enclose an azimuthal angle $\Delta\phi=0$ or $\Delta\phi=\pi$. The states of right and left circular polarization are denoted $|\sigma_\pm\rangle$.

In general, the state Eq. (17) is an entangled (i.e., nonfactorizable) state of the two photon polarizations. The entanglement can be quantified by the von Neumann entropy E . For $|ss\rangle$ or $|tt\rangle$ we obtain $E=\log_2(1+x_1x_2)-x_1x_2\log_2(x_1x_2)/(1+x_1x_2)$, where $x_i=\cos^2(\theta_i)$. Note that only the emission of both photons perpendicular to the plane ($\theta_1=\theta_2=0$) results in maximal entanglement ($E=1$) since only in this case $|+1,\theta_i\rangle$ is orthogonal to $|-1,\theta_i\rangle$. In particular, the two photons are not entangled ($E=0$) if at least one of them is emitted in-plane ($\theta_i=\pi/2$). To observe the proposed effect, the relaxation rate to the biexciton ground state must exceed the biexciton recombination rate. That such a regime can be reached is suggested by experiments with low excitation densities, see, e.g., Refs. 29,30. Then, an upper limit for the pair production rate is given by $(\tau_X+\tau_{XX})^{-1}$, where $\tau_{X,XX}$ is the (bi)exciton lifetime. If a double dot consists of two *nonidentical* QDs, the lowest electron levels can be tuned into resonance by means of an external local electric field, which is sufficient for the generation of entangled photons (or entangled electrons) if the optical selection rules apply. It is then possible that the two photons emitted from different dots differ in energy more than in the previous case with identical dots or if only a single QD (Refs. 4,5) is used. This would facilitate the separation of the two photons with respect to their wavelength, e.g., by means of a low- Q cavity.

Conversely, spin-entangled electrons can be produced by optical absorption followed by relaxation of the biexciton to its ground state. After each QD has been filled with an exciton, the recombination can be suppressed by an electric field. Having removed the holes, the electron singlet and triplet could then in principle be distinguished by a subsequent interference experiment.³¹

We thank A. V. Khaetskii, A. Imamoglu, and P. Petroff for discussions. We acknowledge support from the NCCR Nanoscience, Swiss NSF, DARPA, and ARO.

¹C.H. Bennett and D.P. DiVincenzo, Nature (London) **404**, 247 (2000).

²D. Loss and D.P. DiVincenzo, Phys. Rev. A **57**, 120 (1998).

³P. Recher, E.V. Sukhorukov, and D. Loss, Phys. Rev. B **63**, 165314 (2001).

⁴O. Benson *et al.*, Phys. Rev. Lett. **84**, 2513 (2000).

⁵E. Moreau *et al.*, Phys. Rev. Lett. **87**, 183601 (2001).

⁶F. Troiani, U. Hohenester, and E. Molinari, Phys. Rev. B **62**, R2263 (2000).

⁷P. Chen, C. Piermarocchi, and L.J. Sham, Phys. Rev. Lett. **87**, 067401 (2001).

⁸G. Chen *et al.*, Science **289**, 1906 (2000).

⁹L. Quiroga and N.F. Johnson, Phys. Rev. Lett. **83**, 2270 (1999).

¹⁰M. Bayer *et al.*, Science **291**, 451 (2001).

¹¹E. Biolatti *et al.*, Phys. Rev. B **65**, 075306 (2002).

¹²A.I. L. Efros and A.L. Efros, Fiz. Techn. Poluprovod. **16**, 1209 (1982) [Sov. Phys. Semicond. **16**, 772 (1982)].

¹³L. Banyai *et al.*, Phys. Rev. B **38**, 8142 (1988).

¹⁴T. Takagahara, Phys. Rev. B **39**, 10 206 (1989).

¹⁵G.W. Bryant, Phys. Rev. B **41**, 1243 (1990).

¹⁶Y.Z. Hu *et al.*, Phys. Rev. Lett. **64**, 1805 (1990); Phys. Rev. B **42**, 1713 (1990).

- ¹⁷S.V. Nair and T. Takagahara, Phys. Rev. B **55**, 5153 (1996).
¹⁸P. Hawrylak, Phys. Rev. B **60**, 5597 (1999).
¹⁹A. Kiraz *et al.*, Phys. Rev. B **65**, 161303 (2002).
²⁰C. Santori *et al.*, Phys. Rev. B **65**, 073310 (2002).
²¹G. Schedelbeck *et al.*, Science **278**, 1792 (1997).
²²E. Johnston-Halperin *et al.*, Phys. Rev. B **63**, 205309 (2001).
²³W.F. Brinkman, T.M. Rice, and B. Bell, Phys. Rev. B **8**, 1570 (1973).
²⁴R.J. Luyken *et al.*, Physica E (Amsterdam) **2**, 704 (1998).
²⁵T. Lundstrom *et al.*, Science **286**, 2312 (1999).
²⁶G. Burkard, D. Loss, and D.P. DiVincenzo, Phys. Rev. B **59**, 2070 (1999).
²⁷D. Gammon *et al.*, Science **273**, 87 (1996).
²⁸O. Gywat, G. Burkard, and D. Loss (unpublished).
²⁹B. Ohnesorge *et al.*, Phys. Rev. B **54**, 11 532 (1996).
³⁰E. Dekel *et al.*, Phys. Rev. B **61**, 11 009 (2000).
³¹G. Burkard, D. Loss, and E.V. Sukhorukov, Phys. Rev. B **61**, R16 303 (2000).